GALICS. II: the [α/Fe]-mass relation in elliptical galaxies

A. Pipino[1], J. E. G. Devriendt[1,2], D. Thomas[3], J. Silk[1], and S. Kaviraj[1]

[1] Astrophysics, University of Oxford, Denys Wilkinson Building, Keble Road, Oxford OX1 3RH, UK
   e-mail: axp@astro.ox.ac.uk; pipino@usc.edu
[2] Observatoire Astronomique de Lyon, 9 avenue Charles André, 69561 Saint Genis Laval Cedex, France
[3] Institute of Cosmology and Gravitation, University of Portsmouth, Mercantile House, Hampshire Terrace, Portsmouth,
   PO1 2EG, UK

ABSTRACT

Aims. We test whether the mass- and σ-[α/Fe] relations in the stellar populations of early-type galaxies can be reproduced by a cosmologically motivated assembly history for spheroids.
Methods. We implement a detailed treatment for the chemical evolution of H, He, O, and Fe in GalICS, a semi-analytical model for galaxy formation that successfully reproduces basic low- and high-redshift galaxy properties. We take the contribution of supernovae into account (both type Ia and II), as well as low- and intermediate-mass stars, to chemical feedback. The model predictions are compared with the most recent observational results.
Results. We find that the model shows significant improvement at the highest masses with respect to previous work, where the most massive galaxies were also the most α-depleted. In fact the predicted [α/Fe] ratios in this regime are now marginally consistent with observed values. We show that this result comes from the implementation of AGN quenching of star formation in massive haloes. However, this does not help with the creation of the mass-metallicity relation. Instead, at intermediate masses, the scatter in the predicted [α/Fe] ratios is much larger than the observed dispersion. This problem is related to inadequacies of the model in treating satellite galaxies. In particular, we find an excess of low-mass strongly α-enhanced satellites.
Conclusions. The final stellar [α/Fe] of a single galaxy is determined by the star formation history summed over all the progenitors. In particular, a longer duration the integrated star formation history leads to a lower α-enhancement, as might be expected from the results of closed box chemical evolution models. However, non-negligible differences between closed box and hierarchical model predictions are found, due to processes such as dry mergers and hot gas-phase metal recycling in the latter case. These processes help to build up the galactic mass while keeping the α element abundance in the stars at a super-solar level. To match the observed mass-[α/Fe] relation at low and intermediate masses, we suggest that the next generation of semi-analytical model should feature either stellar or AGN feedback schemes that allow galaxies to self-regulate their own star formation history, rather than being crudely linked to the halo mass. At the same time, mechanisms that allow the very old and passively evolving satellite galaxies that do not merge to accrete fresh gas and form stars at later times should be implemented.

Key words. galaxies: elliptical and lenticular, cD – galaxies: abundances – galaxies: formation – galaxies: evolution – galaxies: stellar content

1. Introduction

The cold dark matter (CDM) scenario (Peebles 1982) successfully explains the growth of the large-scale structure of the universe (Springel et al. 2006). Since, the original attempts to model the galaxy formation process within the CDM framework (Kauffmann & White 1993; Cole et al. 1994), several modifications to the assembly of the baryonic building blocks have been introduced to deal with the complexity of gas physics. Among the main open issues, we mention the anti-hierarchical behaviour of the AGNs (e.g. Hasinger et al. 2005), the evolution of luminosity function with redshift (e.g. Bundy et al. 2005), and the increase in mean stellar [α/Fe] with galaxy mass (or σ) in elliptical galaxies (e.g., Worthey et al. 1992; Trager et al. 2000; Thomas et al. 2005; Nelan et al. 2005; Bernardi et al. 2006; Graves et al. 2007). This relationship, together with the old inferred ages, implies that more massive ellipticals formed earlier and faster with respect to smaller objects (Matteucci 1994; Thomas et al. 2005).

Thomas (1999) and Thomas & Kauffmann (1999) were the first to study the chemical enrichment of α and Fe-peak elements in the framework of hierarchical models of galaxy formation. In

a very simplistic approach, Thomas (1999) ran chemical evolution simulations over the star formation histories predicted by Kauffmann (1996). However, he neglected the complex merger history of the galaxies and modelled the galaxies in the closed box approximation. It turned out that the predicted star formation histories of massive elliptical galaxies were too extended to produce α/Fe ratios consistent with observations. This conclusion was later reinforced by Nagashima et al. (2005), who include a self-consistent treatment of chemical enrichment in semi-analytic galaxy formation models.

More recently, a plethora of new models have been presented (e.g. Croton et al. 2006; De Lucia et al. 2006; Bower et al. 2006; Cattaneo et al. 2005; Sommerville et al. 2008; Fontanot et al. 2007), and one of the key new ingredients in these models is feedback from super massive black holes, which either suddenly halt the star formation by triggering a wind or suppress residual star formation at later times in the so-called "radio mode" (Croton et al. 2006; Bower et al. 2006), thus controlling the evolution of massive galaxies (Granato et al. 2004). Such a scenario seems to be supported by observations at both high (e.g. Nesvadba et al. 2006) and low redshifts

(Schawinski et al. 2007, 2009). The preferred mechanism for the assembly of massive spheroids is a sequence of dissipation-less (*dry*) mergers (e.g. Kochfar & Burkert 2003). For instance, dry mergers are invoked to explain the so-called boxy ellipticals (e.g., Naab et al. 2006) and linked to the evolution of the most massive galaxies, including the brightest cluster galaxies (e.g. De Lucia & Blaizot 2007). In practice, mass assembly still occurs at late times in these models, whereas most of the stars have been formed at high redshift in small sub units. However, according to other studies (e.g. Cimatti et al. 2006), star formation and galaxy assembly could have occurred together at high redshift. In fact, the most massive elliptical galaxies ($L > L_*$), seem to be in place and do not show any signs of significant evolution in mass since $z \sim 1$ (Scarlata et al. 2006).

As the [α/Fe]-mass relation has not been studied in these new generation models, and since they differ in many respects (e.g. via the adopted cosmology, the merger trees, the star formation histories) from the work on which Thomas (1999) based his analysis, the aim of this paper is to fill this gap.

To this end we implement a fully self-consistent treatment of chemical evolution, which includes a robust estimate of the type Ia supernova rate and of Fe production in GalICS (Hatton et al. 2003, Paper I hereafter), a state-of-the-art semi-analytical model for galaxy formation, and evolution based on CDM-driven growth of the structures. Our main goal is to check model predictions against the latest observational results for the α/Fe-mass relation and the mass-metallicity relation (MMR, e.g. Faber 1973; Bender et al. 1993; Trager et al. 2000; Thomas et al. 2005; Nelan et al. 2005; Bernardi et al. 2006; Gallazzi et al. 2006; Graves et al. 2007), that so far could be simultaneously accounted for only by numerical models based on the "revised monolithic" approach (Pipino & Matteucci 2004, PM04). The new results will be then interpreted in the light of our previous work with the chemical evolution models (Thomas 1999; PM04).

The structure of the paper is as follows: the main improvements with respect to Paper I are given in Sect. 2; in Sect. 3 the chemical evolution scheme is tested against the Milky Way and the local ellipticals SNIa rate. In Sects. 4−6 the results are presented and discussed, respectively. Conclusions are given in Sect. 7.

2. The model

2.1. The GalICS galaxy formation model

GalICS is a model of hierarchical galaxy formation which combines high resolution cosmological N-body simulations to describe the dark matter content of the Universe with semi-analytic prescriptions to follow the physics of the baryonic matter. GalICS has been thoroughly presented in Paper I, which we refer the reader to for a detailed discussion of the model assumptions and properties. It has already been used for the study of the colour−magnitude relation and the progenitor bias of elliptical galaxies (Kaviraj et al. 2005), the reproduction of the Galex NUV-optical colours (Kaviraj et al. 2007), and the black-hole mass – σ relation (Cattaneo et al. 2005). It has also been used to explore the consequences the halo-quenching mechanism (Keres et al. 2005) by Cattaneo et al. (2008, and references therein). The above mentioned papers represent a comprehensive set of benchmark tests that we will not repeat here, but simply point out that results are preserved to a large extent in our present implementation. We adopt the Paper I model set-up, unless otherwise stated.

We briefly summarize the specifications of the cosmological N-body simulation used to construct the halo merger trees. This simulation is a realization of a flat cold dark matter universe with a cosmological constant $\Omega_\Lambda = 0.667$. The simulated volume is a cube of side $L_{\rm box} = 100 \, h_{100}^{-1}$ Mpc, with $h_{100} \equiv H_0/100 \, {\rm km \, s^{-1}} = 0.667$, which contains 256^3 particles of mass $8.3 \times 10^9 \, M_\odot$ each, and the cold dark matter power spectrum was normalised in agreement with the present day abundance of rich clusters ($\sigma_8 = 0.88$). One should bear in mind that the dark matter simulation cannot resolve haloes less massive than $1.6 \times 10^{11} \, M_\odot$, which implies that a galaxy less massive than $2 \times 10^{10} \, M_\odot$ is formally below our resolution limit.

As hot gas cools and falls to the centre of its dark matter halo, it settles in a rotationally supported disc. According to Paper I, if the specific angular momentum of the accreted gas is conserved and starts off with the specific angular momentum of the dark matter halo, we assume it forms an exponential disc with scale length $r_{\rm d}$ given by (Mo et al. 1998):

$$r_{\rm d} = \frac{\lambda}{\sqrt{2}} R_{200}. \tag{1}$$

Galaxies remain pure discs if their disc is globally stable (i.e. $V_{\rm c} < 0.7 \times V_{\rm tot}$ where $V_{\rm tot}$ is the circular velocity of the disc-bulge-halo system ; see e.g. van den Bosch et al. 1998), and they do not undergo a merger with another galaxy. In the case where a significant merger occurs, we employ a recipe to distribute the stars and gas in the galaxy between three components in the resulting, post-merger galaxy, that is the disc, the bulge, and a star-burst (see Paper I). In the case of a disc instability, we simply transfer the mass of gas and stars necessary to make the disc stable to the burst component, and compute the properties of the bulge/burst in a similar fashion to that described in Paper I. Recent discussions (e.g. Athanassoula 2008) point out that the creation (if any) of a *classical* bulge by means of disc instability may be not so straightforward. The exploration of newer recipes is beyond the scope of the paper. However, a newer and more accurate criterion for disc stability could affect the fraction of bulge-dominated systems predicted by GalICS and the properties of their stellar populations. Bulges are assumed to have a density profile given by Hernquist (1990). The bulges are assumed to be pressure supported with a characteristic velocity dispersion σ, computed at their half-mass radius.

In Paper I galaxy morphologies are predicted according to the ratio of B-band luminosities of the disc and the bulge components because this ratio correlates well with Hubble type (Simien & De Vacoulers 1986). In particular, the galaxy morphology in the model is determined by the ratio of the B-band luminosities of the disc and bulge components. A morphology index is defined as

$$I = \exp\left(\frac{-L_{\rm B}}{L_{\rm D}}\right). \tag{2}$$

Then, following the analysis of observed galaxies made by Baugh et al. (1996), their classification via the index I, is translated into morphological classes by assuming ellipticals have $I < 0.219$, S0s have $0.219 < I < 0.507$, and spirals have $I > 0.507$. By construction, a pure disc has $I = 1$, whereas a pure bulge has $I = 0$. According to Paper I (to which we refer for a detailed comparison with observations), the morphological mix predicted by GalICS is E:S0:SP+Irr = 17:16:67. This simple prescription is clearly incapable of capturing the complex spectrum of real galaxy morphologies. Therefore, in what follows, we will refer to galaxies with a dominant spheroidal

component when $I < 0.507$, whereas "spirals" refer to *all* other systems. Observationally, the latter group includes not only systems with distinctive spiral morphologies, but also peculiar or irregular systems.

2.2. Chemical evolution

The main novelty of the present version of GalICS is the implementation of a self-consistent treatment of the chemical evolution with finite stellar lifetimes and both type Ia and type II supernovae ejecta. In practice, we follow the chemical evolution of only four elements, namely H, He, O and Fe. This set of elements is good enough to characterise our simulated elliptical galaxy from the chemical evolution point of view as well as small enough in order to minimise computational resources. In fact, [O/Fe] ∼ [α/Fe] ratio, since O is by far the most important α element. Such a ratio is a powerful estimator of the duration of star formation (Matteucci & Greggio 1986) and it will be the primary constraint used in our analysis. Also, the reader should remember that O is the major contributor to the total metallicity, therefore its abundance summed with Fe is a good tracer of the total (i.e. summed over all elements but H and He) metal abundance Z.

In the following the [α/Fe] ratio will always refer to the V-band luminosity-weighted average over the stellar populations that make a galaxy, unless stated otherwise. This value guarantees a robust comparison with its observational counterpart, namely to the "SSP-equivalent" value inferred from the integrated spectra of elliptical galaxies. We refer to Pipino et al. (2006) for details and caveats on the use of "SSP-equivalent" abundances and abundance ratios as proxies for the mean properties of a composite stellar populations like an elliptical galaxy. Here we just mention the main, well-known, problems of the interpretation of the data by reducing the complexity of a spectrum to a SSP. First of all – and even for an actual SSP – one should take into account the *age-metallicity degeneracy*, namely stronger absorption features in the spectra can arise either because a stellar population is old or because it is rather metal rich. Moreover, since luminosity-weighted quantities are strongly affected by the presence of a small fraction of young stars, they do not always reflect the mean age and composition of the bulk of the population.

The star formation rate in the disc is

$$\psi(t) = \frac{M_{\mathrm{cold}}}{\beta_* t_{\mathrm{dyn}}} \, . \tag{3}$$

Here M_{cold} is the mass of the gas in the disc (all the gas in the disc is cold and all the gas in the halo is hot) and t_{dyn} is the dynamical time (the time to complete a half rotation at the disc half-mass radius). The star formation law (Eq. (3)) has the same form and uses the same efficiency parameter β_* for all three components when we redefine M_{cold} as the mass of the gas in the component and t_{dyn} as the dynamical time of the component. For the components described by a Hernquist profile, the dynamical time is $t_{\mathrm{dyn}} = r_{0.5}/\sigma$, where $r_{0.5}$ is the half-mass radius and σ is the velocity dispersion at the half-mass radius.

The parameter β_*, which determines the efficiency of star formation has the same fiducial value of $\beta_* = 50$ (Guiderdoni et al. 1998) adopted in Paper I. However, we identify the SF recipe as one of the prescriptions which one can improve upon. For instance, a short (10^6–10^7 yr) super-Eddington phase in the growth of the central black hole can provide the accelerated triggering of star formation by means of black hole positive feedback (Silk 2005; Pipino et al. 2009). In a sense, GalICS already

turns gas into stars at the maximum possible rate during the merger-induced star-burst phase. A direct implementation of the above recipe will be tested in the forthcoming version of GalICS.

A Salpeter (1955) initial mass function (IMF) that is constant in time over the range 0.1–$40\,M_\odot$ is assumed for the sake of simplicity and to allow a comparison with previous work (Thomas 1999, PM04) and with elemental abundances inferred from observations (Thomas et al. 2007). We warn the reader that several observational studies in the literature point out problems related to the Salpeter IMF; such as, for instance, the over-prediction of the M/L ratio in ellipticals (e.g. Humphrey et al. 2006). These claims find support in theoretical efforts to study the origin of the IMF (e.g. Kroupa 2007). Nevertheless, PM04 showed that the majority of the photochemical properties of an elliptical galaxy can be reproduced with this choice for the IMF and only a slight modification below 1 $M_\odot$ may be required to solve the above mentioned issues (e.g. Renzini 2005). Such a modification does not affect the predicted abundance ratios (Thomas 1999). Also, note that a flatter IMF has been used by Nagashima et al. (2005). In particular, their galaxies could achieve a supersolar alpha/Fe ratio only when a top-heavy IMF was adopted during merger-induced starburst. However such an assumption is not enough (in the context of hierarchical mergers) to reproducing the correct α/Fe-mass relation. Therefore we do not repeat the exercise here. We expect that a flattening of the IMF regardless of the galaxy mass leads to a overall shift towards higher values of the predicted [α/Fe] ratio, but does not affect the slope of the α/Fe-mass relation unless one finds a good reason to make the IMF flatter as the galactic mass increases (as for the integrated galactic IMF, Weidner & Kroupa 2005). However, this modification alone seems not to suffice, as recently shown by Recchi et al. (2009).

We adopted the yields from Iwamoto et al. (1999, and references therein) for both SNIa and SNII. The reader should note that a change in the stellar yields will introduce a systematic offset of a few tenths of a dex in the model predictions (see Thomas et al. 1999, PM04), hence it might leave room for some fine-tuning for a suitable choice of stellar nucleosynthesis[1]. However, being only an offset, this change cannot create nor modify the slope of the predicted α/Fe-mass relation. But, most importantly, the successful calibration of our model with element ratios observed in Milky Way stars (see below) does not allow significant modifications of the underlying stellar yields.

The SNIa rate for a SSP formed at a given time is calculated assuming the single degenerate scenario and the Matteucci & Recchi (2001) Delay Time Distribution (DTD). The convolution of this DTD with ψ (see Greggio 2005) gives the total SNIa rate, according to the following equation:

$$R_{Ia}(t) = k_\alpha \int_{\tau_i}^{\min(t,\tau_x)} A(t-\tau)\psi(t-\tau)\mathrm{DTD}(\tau)\mathrm{d}\tau \tag{4}$$

where $A(t-\tau)$ is the fraction of binary systems which give rise to type Ia SNe. Here we will assume it is constant (see Matteucci et al. 2006, for a more detailed discussion). The time τ is the delay time defined in the range (τ_i, τ_x) so that:

$$\int_{\tau_i}^{\tau_x} \mathrm{DTD}(\tau)\mathrm{d}\tau = 1 \tag{5}$$

---

[1] For instance by: i) extending the upper mass limit of the IMF to 100 $M_\odot$; ii) neglecting the ejecta of the stars in the mass range 8–11 $M_\odot$ (whose O/Fe is slightly sub-solar); iii) setting the SNIa rate to the lowest value permitted by observations.

where τ_i is the minimum delay time for the occurrence of type Ia SNe, in other words the time at which the first SNe Ia start occurring. We assume that τ_i equals the lifetime of a 8 $M_\odot$ star, while for τ_x, which is the maximum delay time, we assume the lifetime of a 0.8 $M_\odot$ star. Finally, k_α is the number of stars per unit mass in a stellar generation and contains the IMF. The detailed treatment of SNIa is a substantial improvement with respect to Paper I.

The simulation produced 70 output snapshots spaced logarithmically in the expansion factor from $z = 100$ to 0. This implies that the snapshots are taken at $50-100$ Myr intervals at redshifts above 3 and at 200 Myr intervals at later times. Stars – and baryonic processes at the galactic scale that need finer detail – are evolved between time-steps using sub-stepping of at least 1 Myr. During each sub-step, stars release mass and energy into the interstellar medium. In GalICS, the enriched material released in the late stages of stellar evolution is mixed to the cold phase, while the energy released from supernovae is used to re-heat the cold gas and return it to the hot phase in the halo. The re-heated gas can also be ejected from the halo if the potential is shallow enough (see also Paper I). The rate of mass loss in the supernova-driven wind that flows out of the disc is directly proportional to the supernova rate (see below).

The original formula for the chemical processing of the total metal content (see Paper I) has been extended to the elemental species we deal with, so that the ejecta in the gas mass from the stellar population are:

$$\mathcal{E}_i(t) = \int_{m(t)}^{\infty} \psi(t-t_m)([m-w(m)]Z_{i,\text{cold}}(t-t_m)+mY_i(m))\phi(m)\mathrm{d}m \quad (6)$$

where $m(t)$ is the mass of a star having lifetime t_m, $w(m)$ is the mass of the remnant left after the star has died, and $\phi(m)$ is the IMF. The first term on the right hand side represents the re-introduction of unprocessed metals in the stars when they formed, and $Y_i(m)$ is the fraction of the initial stellar mass transformed via stellar nucleosynthesis into the element i. Throughout this work, we assume chemical homogeneity (instantaneous mixing), such that outflows caused by feedback processes are assumed to have the same metallicity as the interstellar medium, though in reality the situation cannot be captured by our simple recipe (Strickland & Heckman 2009) and newly produced metals are more likely to be ejected than the gas (e.g. Recchi et al. 2004). Note that, thanks to the fine sub-stepping used for the stellar evolution, also ejecta from SNII and the contributions of single low-mass stars is implemented without the need to assume the istantaneous recycling approximation.

2.3. Galaxy evolution and properties

The fundamental assumption is that all galaxies are born as discs at the centre of a dark matter halo. The transformation of disc stars into bulge stars and of disc gas into star-bursting gas is due to bar instabilities and mergers. The star-bursting gas forms a young stellar population that becomes part of the bulge stellar population when the stars have reached an age of 100 Myr. We do not readjust the bulge radius when this happens. The starburst scale is $r_{\text{burst}} = \kappa r_{\text{bulge}}$ with $\kappa = 0.1$.

The fraction of the disc mass transferred to the spheroidal component (the bulge and the star-burst) depends on the mass ratio of the merging galaxies. Separation between a minor and a major merger is defined to be for a mass ratio of 1:3.

According to Paper I, during a merger a fraction X of gas and stars originally sitting in the disc remain in the disc. The rest of the gas from the disc goes into the starburst, as well as its stars. Any stars that were already in the bulge stay in the bulge, but all the gas is consumed in the starburst. All the material (gas and stars) that was originally in a starburst remains in that starburst. Note that gas is never added to the bulge in this process, but that a small amount of gas is generally present in the bulges, coming from stellar mass loss.

2.4. Energetics

The SNII feedback is given by:

$$\dot{m} = 2\psi(t)\frac{\epsilon \eta_{\text{SN}} E_{\text{SN}}}{v_{\text{esc}}^2} \quad (7)$$

where ϵ is the efficiency of the supernova-triggered wind which is proportional to v_{esc}^2 and depends both on the porosity of the ISM (see Silk 2001, for details) and the mass-loading factor. This latter accounts for entrainment of interstellar gas by the wind and can be considered as a free parameter whose value is around 10. Note that in the previous equation, η_{SN} is the number of supernovae per unit star-forming mass, which is a prediction of the IMF chosen, and E_{SN} is the energy of a supernova, assumed to be 10^{51} erg.

Equation (7) is applied to find the fraction of gas in the ISM that is lost by the galaxy and ejected in the intra halo medium. We then equate the fraction of this gas that is completely ejected from the halo, to the galaxy/halo escape velocity ratio. The gas ejected from the halo is added to the halo reservoir where it may subsequently be accreted. There is no specific timescale for such accretion to occur. In Paper I it is assumed that, when the halo subsequently accretes dark matter from the background, some of this dark matter will carry "primordial" baryons (i.e with the baryon fraction Ω_b, and zero metallicity), and the rest will have the same baryon fraction and metal content as that of the halo reservoir, up to the point where the reservoir is fully used up. In Paper I this effect is parametrized with the halo recycling efficiency $\zeta = 0.3$ (see Hatton et al. 2003, for details).

In contrast to chemical evolution models as PM04, where the total Ia+II SNe feedback is sufficient to halt the SF, Paper I relies onto the observed correlation between black-hole mass and velocity dispersion (Ferrarese & Merrit 2000; Gebhardt et al. 2000), and simply mimics the AGN feedback by preventing the gas from cooling in a halo which has a mass above the critical value of ~10^{12} $M_\odot$ to quench cold gas accretion. Another halo-quenching mechanism has been implemented into GalICS by Cattaneo et al. (2008), who showed how this further refinement leads to a better agreement between our model predictions and SDSS observations of the luminosity function and the colour bimodality (Baldry et al. 2004). We also tested models in which we implemented Cattaneo et al.'s recipe. Since this modification does not significantly change our findings we will present the results obtained with the original Hatton et al. (2003) model.

3. Calibration of the model

To provide a consistency check for our model, we adopt a procedure typical of chemical evolution studies. We first compare MW-like galaxies in our simulations with the known properties of our galaxy. We, then, check that the predictions of the present-day SNIa in both spiral and elliptical galaxies match the observed values.
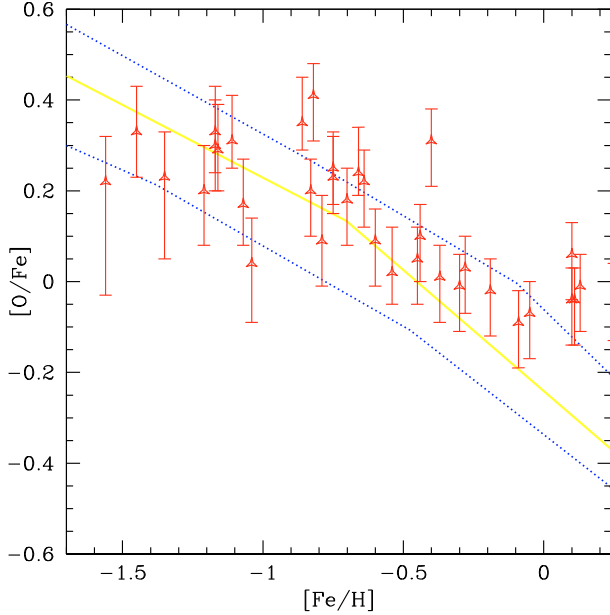
Fig. 1. The solid line shows the average [O/Fe] as a function of [Fe/H] as predicted by GalICS for a MW-like spirals. The dotted lines bracket the region where GalICS predictions are. Triangles: observational data for individual stars in the MW disc as compiled and homogenised by François et al. (2004).

3.1. Comparison to the abundances in the stars of the Milky Way

Since many properties of such galaxies have already been tested in the calibration of Paper I, here we use the same selection criteria for MW-like galaxies namely $m_{gas}/m_{bar} = 0.10 \pm 0.05$, $M_K = -23.7$ mag ± 0.3 mag, $V_c = 220 \pm 20$ km s^{-1} (V_c is the circular velocity of the disc, and the material is assumed to have purely circular orbits). Obviously we require that the galaxy has spiral morphology. Here we focus only on the chemical evolution predictions. We found that ∼3% of the spiral population is produced by MW-like objects in agreement with Paper I statistics.

In Fig. 1 we compare the [O/Fe] ratio as a function of [Fe/H] *in the stars* of the MW-like spirals predicted by GalICS to observations. As the metallicity in the range $[-1.5, 0]$ pertains to the typical composition of the MW disc stars, and since GalICS cannot model MW halo stars, we show the predictions only for the disc component of the MW-like galaxies. The points are observations for individual stars in the MW disc taken from the compilation by François et al. (2004), whereas the solid line give the typical predicted trend, averaged over the model galaxies. The dotted lines bracket the region of the plane [Fe/H]−[O/Fe] where ∼90% of our model predictions lie. The agreement with the overall trend observed in our own Galaxy makes us confident that the model is correctly calibrated. Unfortunately, due to the metallicity resolution (five bins in total metallicity Z, namely 0.001, 0.004, 0.008, 0.02 and 0.04) of the code and the fact that galaxies are identified only once their host DM haloes are quite massive ($M_{vir} > 1.6 \times 10^{11} M_\odot$), we cannot explore the region at [Fe/H] < −1.5.

3.2. Present-day SNIa rate

We now verify that the model galaxies predict a present-day morphology-dependent SNIa rate in agreement with observations. The MW-like spirals presented above exhibit a SNIa rate
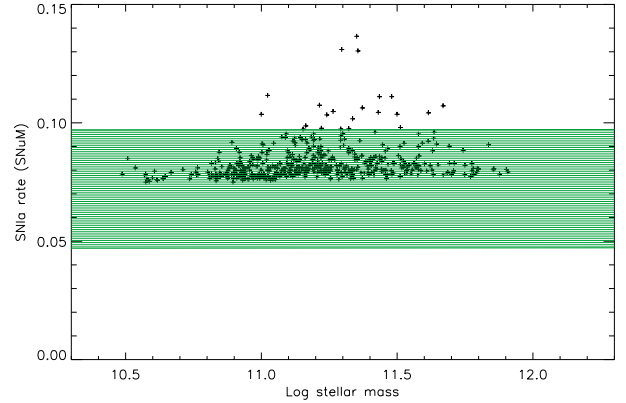
Fig. 2. Present-day SNIa rate in SNuM units as a function of the galactic mass for our model ellipticals (black crosses). The hatched region outlines the 1σ dispersion region around the observational best fit (0.066 SNuM, Mannucci et al. 2008) to SNIa in ellipticals only.

of 0.09 SNuM (i.e. specific SN explosion rate in units of $10^{10} M_\odot$ of stars per century), which is in fair agreement with the observational estimates ($0.06^{+0.019}_{-0.015}$ for S0a/b and $0.14^{+0.045}_{-0.035}$ for Sbc/d, respectively, see Mannucci et al. 2008) given the fact the GalICS does not allow a finer morphological classification. In particular, in order to reproduce the present-day observed SNIa rate, we assume $A = 0.0025$ which is the value typically adopted in chemical evolution models of the Milky Way (see Matteucci et al. 2006).

Once this check is done, we can also compare the prediction for the SNIa rate in ellipticals to the observed rate. As shown in Fig. 2 the vast majority of our simulated ellipticals exhibit a present-day SNIa rate within 1σ from the observational mean value given by Mannucci et al. (2008) for ellipticals. The few objects that have an SNIa rate higher than the observational range in Fig. 2, are intermediate mass galaxies with a luminosity-weighted age lower than 7 Gyr. They experienced a relatively recent star formation with respect to the bulk of the population and, hence, have a higher supernova rate. We will see that they have the lowest [α/Fe] ratios. This test basically guarantees that, given the star formation history of the model galaxies, we have calibrated the uncertainties in the progenitor nature and delay time distribution of SNIa which are incorporated in the parameter A (see Eq. (4)).

As a result, the Fe production rate from SNIa is also calibrated.

4. The σ- and mass-[α/Fe] relations

4.1. Overall trends

From this section onwards we deal with the main novelty of the present work, namely the study of the predicted α/Fe-mass relation and its comparison to observations. To be consistent with observed values, we present luminosity-weighted values which take into account the disc component (if any). We stress, however, that the mass-weighted quantities do not differ much from the luminosity-weighted ones especially at the high mass end of the sample, where star formation has been suppressed at high redshift. Here we present our predictions for the [α/Fe] ratio in the whole galaxy and consistently compare them to the recent observational estimates by Thomas et al. (2007). Thomas et al. (2007) have collected a magnitude-limited sample of 1652 elliptical galaxies in the redshift range $0.05 < z < 0.055$ with
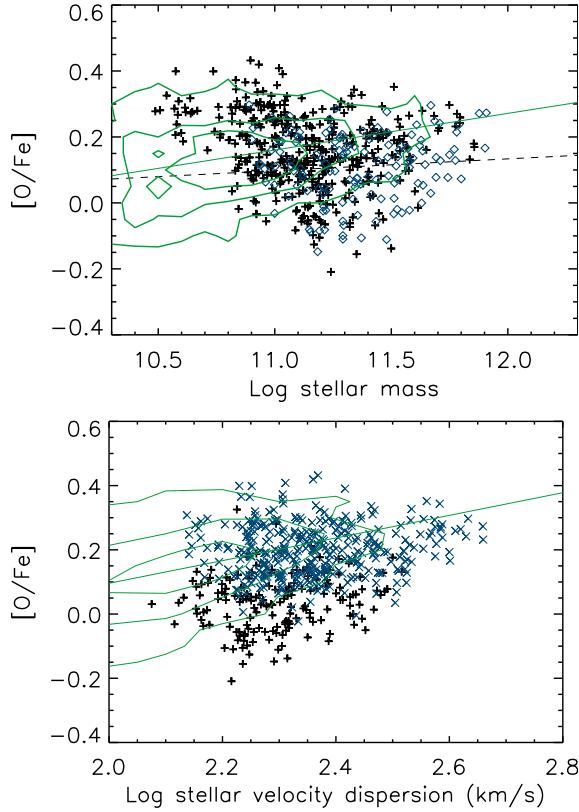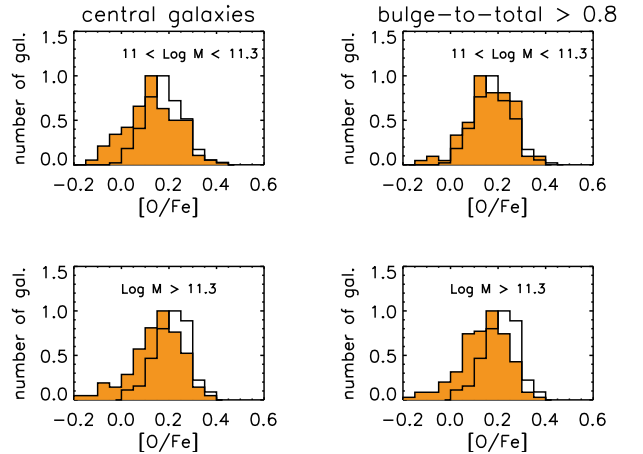
Fig. 3. The α/Fe-mass and -σ relations as predicted by GalICS for the whole sample of ellipticals (points). Contours: observations by Thomas et al. (2007) along with a linear fit to them (solid line). *Upper panel*: satellite galaxies (crosses) and central galaxies (diamonds) are marked. A linear fit to the relation for central galaxies is represented by a dashed line. *Lower panel*: all points: all galaxies predicted by our model. A subsample of ellipticals older than 10 Gyr is emphasised with asterisks.

Fig. 4. Normalized distribution of central galaxies (*left column*) and elliptical galaxies with a bulge to total ratio larger than 0.8 (*right column*, see text) as a function of the [α/Fe] ratio in different mass bins. The hatched histograms refer to our model prediction, whereas the empty histograms are for Thomas et al.'s data. Note the tail at low [α/Fe] in the model predictions not present in the data. Even if the model predictions were able to reproduce the mean [α/Fe] at a given mass, the distributions would still differ.

apparent *r*-band magnitude brighter than 16.8 from the SDSS Data Release 4. The most radical difference with respect to other galaxy samples constructed from SDSS is their choice of pure morphological selection of galaxy type by visual inspection. An important improvement in this approach is that stellar population and emission line templates are fitted simultaneously to the galaxy spectrum. On each spectrum, Thomas et al., then measure the 25 standard Lick absorption line indices following the index definitions of Trager et al. (1998). The stellar population models of Thomas et al. (2003, 2004) are used to derive luminosity-weighted ages, metallicities, and α/Fe ratios by means of a fit to all 25 indices.

We also note that the observed radial gradient slope in the [α/Fe] has, on average, a null value (e.g. Mehlert et al. 2003; Rawle et al. 2008, from the observational point of view; Pipino et al. 2008, for the models). Hence, any impact on the slope of the [α/Fe]-mass relation because of aperture effects due to the fixed fiber size in the SDSS, is negligible.

The results for our fiducial GalICS version are presented in Fig. 3, where we present our models as points (in particular crosses refer to satellite galaxies, whereas diamonds represent central galaxies) and Thomas et al. (2007)'s data as contours. We also show a fit to the Thomas et al. data by means of a solid line to help the visualization of the mean [α/Fe] at a given mass. We note a factor of 2 offset between our mass scale and the one used by Thomas et al. (2007). This is due to the fact that Thomas et al. derived the dynamical masses from the measure of the line of sight velocity dispersion and how they selected their sample.

We remind the reader that we classify as ellipticals galaxies that have $I < 0.219$. Galaxies with bulge-to-total luminosity ratio larger than, e.g., 0.8 amount to ~50% of the points shown in Fig. 3. In particular, they typically correspond to central galaxies (diamonds, upper panel of Fig. 3) with mass $>10^{11}$ $M_\odot$. No significant changes in the conclusions for central galaxies are obtained if only these objects are compared to observations (cf. Fig. 4).

We notice that the most massive galaxies attain a typical level of α-enhancement that is only 1σ off (below) the value suggested by the observations at a given mass. This is an improvement with respect to the situation depicted by Thomas (1999) and Nagashima et al. (2005), where the most massive galaxies harboured the most α-depleted stellar populations. As we will see in Sect. 4.2, fundamental ingredients are the fact that i) these galaxies assemble through dry (gas-poor) mergers and ii) assemble most of their mass over a very short time-scale. Indeed, this ensures that the pollution from SNIa is kept at a low level and, hence, that they maintain a super-solar [α/Fe] ratio in their stars. In order to meet condition *i)*, low-mass and highly α-enhanced building blocks are needed at high redshift. Indeed, GalICS predicts that a small number of these (crosses in the upper panel of Fig. 3), with masses $\sim 0.5-1 \times 10^{11}$ $M_\odot$ should survive down to redshift zero. Unfortunately, such galaxies are not observed in such a high number[2]. We will discuss this problem in greater detail in Sect. 6. More massive galaxies tend to be older than lower mass ones (see also Sect. 4.2), in agreement with observations and at variance with Thomas (1999)'s and Nagashima et al. (2005)'s findings.

As far as the [α/Fe]-mass relation for the entire sample is concerned, in agreement with Nagashima et al. (2005), the α/Fe ratios do not show any correlation with mass (Fig. 3, top panel). A linear fit of the simulation results in the [α/Fe]-mass plane would give a flat relationship (excluding the lowest mass objects). Whilst the simulations seem to produce decreasing [α/Fe] ratios with increasing galaxy mass for masses below

---

[2] Also, note that GalICS does not predict low mass satellite galaxies with [α/Fe] equal or lower than the observational mean in that mass regime.
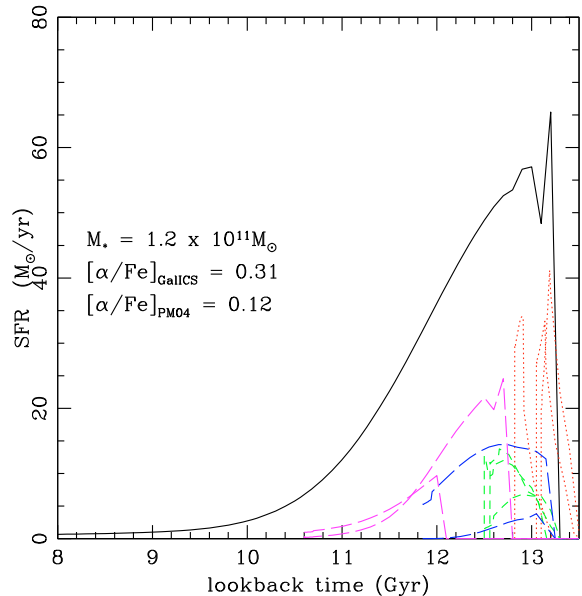
$\sim 2 \times 10^{11}$ $M_{\odot}$, we notice an upturn at the high-mass end, as in the case of central galaxies (diamonds in the upper panel of Fig. 3). However, a linear fit of the [α/Fe]-mass relation for central galaxies would return a positive, yet significantly flatter, trend (dashed line, Fig. 3, top panel). The reader should note that even if we offset our mass scale in order to match the Thomas et al. (2007) one, the slope of the predicted the average trend (dashed line in the upper panel of Fig. 3, see below) will not change. Also, the average α-enhancement at a given mass is lower than the observed value. At intermediate masses, instead, the predicted scatter is larger than the observed one. Finally, central galaxies (diamonds in the upper panel of Fig. 3) do exhibit a somehow smaller scatter than the entire sample of model ellipticals. This happens because the baryonic mass is more strongly correlated with the mass of the DM halo in a fashion similar to the behaviour of the α/Fe-σ relation (lower panel of Fig. 3, see below) than for the rest of the model galaxies. In order to look at the central galaxy properties in more detail, in Fig. 4 we show the normalized distribution of central galaxies (left column) and elliptical galaxies with a bulge to total ratio larger than 0.8 (right column, see above) as a function of the [α/Fe] ratio in different mass slices. The hatched histograms refer to our model prediction, whereas the empty histograms are for Thomas et al.'s data. Note the tail at low [α/Fe] in the model predictions not present in the data. Even if the model predictions were able to reproduce the mean [α/Fe] at a given mass, the distributions would still differ.

Similar results are obtained when plotting the [α/Fe] as a function of the stellar velocity dispersion σ (Fig. 3, bottom panel). Comparing the two panels in Fig. 3, we notice that the scatter is reduced and that the galaxies follow a trend which is closer to the observational results. We can understand this as we expect the velocity dispersion to be more correlated with the properties of the DM host haloes, whereas the baryonic mass is more sensitive to our modelling of feedback processes. However, one should bear in mind that GalICS assumes virialization and a fixed density profile (see Paper I) to calculate σ. Whilst these assumptions are reasonable at $z = 0$, they very likely should be revised at high redshifts.

If we consider the subsample of galaxies whose luminosity-weighted ages are larger than 10 Gyr (lighter asterisks in the lower panel of Fig. 3), we notice the paucity of galaxies populating the region below the observed area in the [α/Fe]-mass plane. We attribute this to the fact that these galaxies live in massive haloes where the original AGN feedback implemented in GalICS halted the cooling in the gas a long time ago. Indeed, by looking at the asterisks in the lower panel of Fig. 3, they seem to better correlate with sigma than the entire population. This is because of the way AGN feedback is modelled. The same is true if we adopt the the halo-quenching mechanism introduced in GaLICS by Cattaneo et al. (2008). This finding confirms the interpretation of the [α/Fe] ratios below the observed range as being related to too long a duration of star formation, as we will discuss below.

Moreover, we note that the scatter is still much larger than the observed one and that, for a given velocity dispersion, the model galaxies tend to have on average a lower [α/Fe] ratio than the observed ones. The latter problem can be handled in several ways[3] (stellar yields, IMF, feedback, SF efficiency), whereas the former is intrinsic to the model and linked to the nature of the

---

[3] Provided that one can still reproduce the [O/Fe]−[Fe/H] trend in the Milky Way with this new choice.

Fig. 5. Integral star formation history for a $\sim 10^{11}$ $M_{\odot}$ galaxy with strong α-enhancement (solid line). The SFH inherited from the single building blocks is also shown by dotted (progenitors merging very early on), dashed (progenitors merging at $z \sim 4$) and long dashed (progenitors merging at $z \sim 2-3$) lines, respectively.

merger process where the scatter in the duration of individual SF histories augments as galaxies merge together.

In order to better understand the origin of this scatter, we now focus on those few selected galaxies with the same mass, but very different [O/Fe] and we study their star formation histories. We perform this exercise for *typical ellipticals* of $\sim 10^{11}$ $M_{\odot}$ but the results apply also to *massive ellipticals* of $\sim 10^{12}$ $M_{\odot}$.

4.2. The star formation history in detail

We present the analysis in the $\sim 10^{11}$ $M_{\odot}$ mass range, where most of the predicted galaxies scatter outside the region of the observed values. A useful test for understanding the behaviour of such galaxies is provided by running chemical evolution models with the same stellar yields, IMF and the same *integral* star formation rate as the selected semi-analytic galaxies. We are aware that the predictions from chemical evolution models that deal with the formation and evolution of single galaxies under the monolithic framework might be very different from the GalICS predictions. For instance, numerical models based on the monolithic approach often lack a background cosmological framework (but see, e.g. Merlin & Chiosi 2006), hence the lack of mergers and differences in feedback are important caveat that the reader should keep in mind. Nevertheless, since the constraints on the duration of the SFH arising from the observed α-enhancement are always inferred by means of a chemical evolution model, it is important to compare the two approaches. Particular care has been dedicated to the fact that both GalICS and the PM04 model have the same IMF, stellar yields, SNIa DTD, namely the main actors as far as the chemical evolution is concerned. In Figs. 5 and 6, we present the integral star formation history (summed over all progenitors) of two galaxies of the same mass as a function of look-back time (solid lines).

In general, the integral star formation history appears to be broader than the one obtained by means of a monolithic collapse which would predict the same [α/Fe] ratio. Indeed when we force the SFH pictured in Fig. 5 (solid line) to happen in a
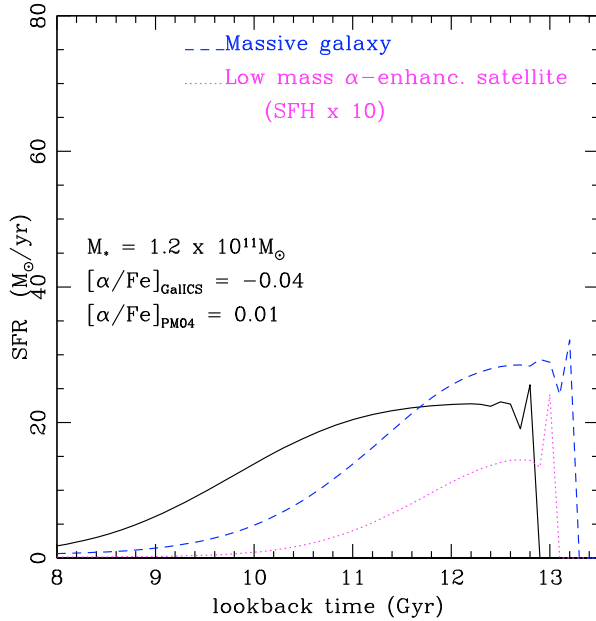
**Fig. 6.** Integral star formation history for a $\sim 10^{11}$ $M_\odot$ galaxy with nearly solar [α/Fe] (solid line). For comparison, we show the SFH for a $\sim 8 \times 10^{11}$ $M_\odot$ galaxy with [α/Fe] = 0.3 (dashed line) and for a low-mass ($\sim 3 \times 10^{10}$ $M_\odot$) strongly α-enhanced satellite (dotted line).

Fig. 7. The α/Fe-mass relation as predicted by GalICS for the whole sample of ellipticals (points). A subsample of ellipticals which experienced at least two mergers is presented as triangles. Contours: data by Thomas et al. (2007).

standard chemical evolution model (PM04), the predicted [O/Fe] is lower by 0.2 dex than that obtained with GalICS. This brings the galaxy from a value of [α/Fe] = 0.31 down to a value of [α/Fe] = 0.12. This partly explains why our results at the high mass end lie closer to the observational values than those in Thomas (1999), who adopted a closed-box chemical evolution model and predicted [α/Fe] as low as 0 for the most massive galaxies. The rest of the difference between Thomas (1999)'s findings and our results is due to the dramatic improvement in the star formation histories predicted by the most recent hierarchical models (cf. Fig. 9, this work, as well as Fig. 10 in De Lucia et al. 2006; or Figs. 5 and 6 in Cattaneo et al. 2008).

The galaxy whose SFH is portrayed in Fig. 5 has 9 progenitors with 4 of them merging very early on (i.e. at $z < 4.7$), and which is passively evolving from red-shift 2. Looking at Fig. 5 (dashed and dotted lines) we see that all the progenitors of this galaxy actually have individual SF time-scales which are shorter than the one that would be inferred from the mass-weighted SFH of the galaxy itself. To better explain this point, we consider the ideal case in which we have only two progenitors with the same masses, similar star formation histories (such that their final [α/Fe] is appropriate for their mass), but assume also that the peak in their star formation rates are shifted by about 1 Gyr (one is younger than the other and this difference in age cannot be detected with the standard line-strength indices technique if these objects are more than 10 Gyr old). Let us also assume that these two galaxies coalesce via a dry merger later in their evolution. The final object has the same [α/Fe] as the progenitors, while its mass is only doubled; hence it still matches the observations, given the spread in the α/Fe-mass relation (Pipino & Matteucci 2008, hereafter PM08). The integral star formation history, instead, will look like the one in Fig. 5, thus broader than the 0.5−0.7 Gyr expected by PM04 (their model II) in order to satisfy the α/Fe-mass relation. This explains why the [α/Fe] ratio calculated by GalICS is higher than the one derived by a pure chemical evolution model of a single object with the same mass-weighted SFH. According to Pipino & Matteucci (2006, PM06),
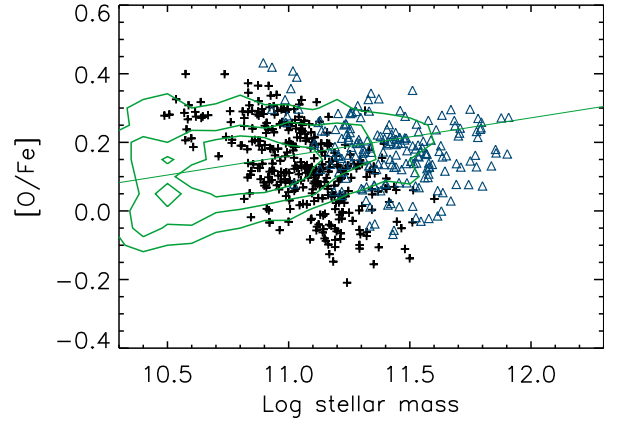
the above example will lead to similar conclusions even if star formation is allowed to occur when the two galaxies merge. PM06 found, in fact that if a starburst triggered by significant accretion of pristine gas (comparable with the mass of stars already formed – roughly similar to a major wet merger in a galaxy formation picture) occurred at a significantly high redshift and just after the main burst of SF, the present day photo-chemical properties of the final elliptical galaxy may match the observed ones.

For the SFH presented in Fig. 6, we have an α-depletion with GalICS which does not occur in PM04. Even though this change is enough to bring the galaxy back within the range of observed values, the discrepancy between the two model predictions is much smaller than in the previous case. The difference here is that we have only one progenitor which explains why the [α/Fe] ratios of GalICS and the pure chemical evolution model are in much better agreement. The small offset is mostly due to the fact that PM04 is a closed box.

For comparison, we also show the SFH for a $\sim 8 \times 10^{11}$ $M_\odot$ galaxy with [α/Fe] = 0.3 (dashed line) and for a low-mass ($\sim 3 \times 10^{10}$ $M_\odot$) strongly α-enhanced satellite (dotted line). For the comparison between a stacked specific (i.e. per unit stellar mass) SFH for galaxies in different mass bins and the observations (e.g. Thomas et al. 2005), we refer to Cattaneo et al. (2008, cf. their Figs. 5 and 6) and we do not repeat the analysis here. We just mention that Cattaneo et al. (2008) show that the average duration of the SFH is shorter in the more massive systems in a way that *resembles* that inferred by Thomas et al. (2005). However, this is not enough to imply a α/Fe-mass relation. On the other hand, with the help of the SFH presented in this section, we explained why the average duration of the SF is a factor of 3−5 longer (and consequently the peak value a factor of 3−5 lower) than that required from pure chemical evolution studies on line-strength indices analysis to reproduce the [α/Fe] in massive ellipticals.

Looking at statistics with the help of Fig. 7 no merger case (crosses) represents 42% of the total number of elliptical galaxies and is biased towards lower masses as we would expect since massive ellipticals are built by multiple mergers in the hierarchical galaxy formation scenario (triangles in Fig. 7 indicate galaxies which experienced at least two mergers.). One might be worried that these results depend on the mass resolution of the *N*-body simulation, however as stated earlier in the paper our mass resolution is such that galaxies more massive
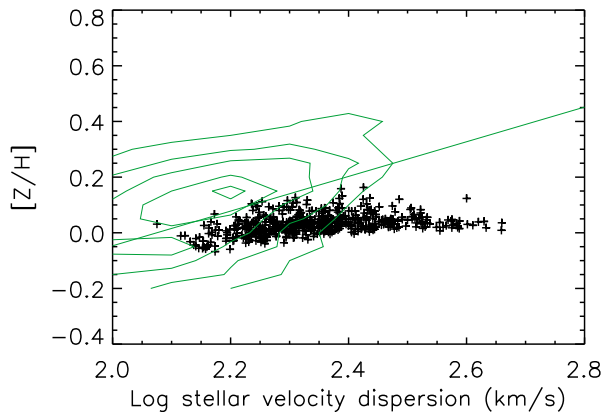
Fig. 8. The MMR as predicted by GalICS for the whole sample of ellipticals (black points). Contours: data by Thomas et al. (2007) along with the linear-regression best fit (solid line). Note that elliptical galaxies exhibit quite strong [Z/H] gradients within one effective radius (e.g Carollo et al. 1993; Davies et al. 1993) and the Thomas et al. (2007) galaxies were observed with a fixed fiber size. Therefore it is difficult to make a meaningful comparison between our predictions and observations as in the case of the [α/Fe]-mass relation (see text).

Fig. 9. The α/Fe-mass relation predicted by GalICS for the whole sample of ellipticals (black points). In this run, the AGN feedback has been switched off. Data as in the previous figures. Note that in this case we have fewer ellipticals than in Fig. 3 simply because gas is allowed to cool onto a disc at the centre of massive DM haloes, which leads us to classify more central galaxies as disc-dominated spirals.

than 2×10^{10} $M_\odot$ are resolved and this mass is about a factor of 10 lower than the mass of ellipticals considered in our analysis.

We also note that in GalICS, the galaxies do not evolve as closed boxes. They instead exchange metals with the surrounding hot halo, and stars originally created in discs can become part of bulges because of instabilities and mergers. Such processes, render the interpretation of the final [α/Fe] ratio on the basis of the SFH alone even more complicated.
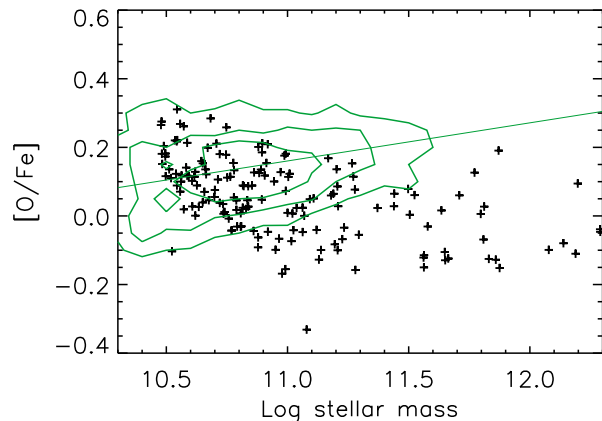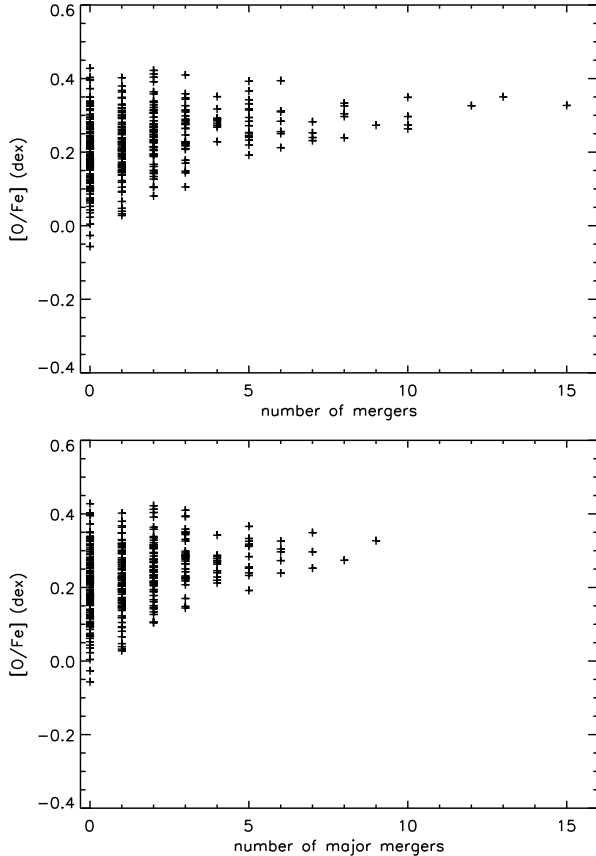
5. The mass-metallicity relation

In Fig. 8 we show the predicted MMR relation against the data by Thomas et al. (2007).

The reader should keep in mind that elliptical galaxies do exhibit quite strong (i.e. −0.3 dex per decade in radius) [Z/H] and [Fe/H] gradients within one effective radius (e.g. Carollo et al. 1993; Davies et al. 1993; Rawles et al. 2008). In practice, given the fixed aperture set by the SDSS fiber size, it is likely that smaller galaxies contributed with most of their light, whereas only the central regions (more metal rich) are observed in bigger galaxies, thus biasing the observed slope of the MMR towards steeper values than the reality. However, a MMR does exist for the central regions of elliptical galaxies (e.g. Thomas et al. 2005). Therefore, the bias, if any, is not sufficient to explain the slope.

A failure in reproducing the MMR is expected on the basis of the preliminary analysis by PM08. In particular, they started with the assumption that, if one wants to create a large elliptical with a suitable α-enhancement by means of a series of exclusively dry-mergers starting from small building blocks, such small objects should have the correct final [α/Fe][4], much higher than required by the observations for their mass. PM08 showed that, as we expect that at least the building blocks can be treated in the monolithic collapse approximation, in order to have a very high [α/Fe], they will have a very low metallicity. Hence, the final outcome of the mergers, namely that the large ellipticals will have a low-metallicity at variance with the observed MMR. Our

models are considerably more complicated than the extreme assumptions used in the PM08 exercise. Nonetheless, the fact that the MMR is not reproduced may hint at i) the need for a more efficient conversion of gas into stars in the progenitors; ii) a lower dilution of metals from pristine gas (which will not affect the abundance ratios); iii) a lower ejection efficiency of metals by SNe feedback. This last solution leads to a worsening of the predicted [α/Fe]-mass relation (see the Discussion), whereas the first one may help with both problems.

We do not show other predictions, such as the age-mass and colour magnitude relations. We refer the reader to Cattaneo et al. (2008) and Kaviraj et al. (2005) who show a remarkable agreement of the predictions made by means of GalICS with the latest observational results. We only note that the predicted scatter in the predicted MMR and (SSP-equivalent) age-mass relationships is comparable to the *intrinsic* scatter derived by Thomas et al. (2005, 2007). On the other hand, the scatter in the α/Fe-mass relation is about twice as big.

6. Discussion

In the previous section, we showed the sensitivity of [α/Fe] to the integral star formation history of the galaxy and estimated the offset in the predicted value with respect to pure monolithic formation. Moreover, we studied the scatter in the predicted [α/Fe]-mass relation at a fixed mass. In order to understand these results, it is important to understand how the quenching mechanism works in GalICS. In order to do this, we present a model in which we switch off the SMBH heating of the intra-halo gas. In this case, we predict that the more massive galaxies are younger than the less massive ones – with a typical age of 6 Gyr (at variance with the observational results) – and that they are strongly α-depleted. As can be seen in Fig. 9, we basically confirm with a more self-consistent model the results that Thomas (1999) obtained. Note, however, that several differences between current models and the model that was used by Thomas (1999), e.g. the cosmological parameters and the merger trees, hamper us from a proper quantitative comparison. Nonetheless it is surprising that our results agree with those by Thomas (1999) and also, again at least from a qualitative point of view, with Nagashima et al. (2005)'s results. Therefore a dramatic improvement in the star formation histories by means of a quenching mechanism is

---

[4] Dry mergers do not change the metallicity and the α-enhancement because they do not trigger star formation.

Fig. 10. α-enhancement versus number total number of mergers (*top panel*) and number of major mergers (*bottom panel*) for our model galaxies.

responsible for the α-enhanced massive galaxies that we predict. On the other hand, in the case without AGN feedback (not shown here), the slope of the predicted mass-metallicity relation is closer to the observed one than in the fiducial case. However, the overall metallicity is lower due to the fact that nothing stops cold gas, hence metal dilution, from being accreted at later times.

Therefore, in order to satisfy the mass-[α/Fe] relation, some kind of SF quenching is needed. The recipe adopted in the present work assumes that only the most massive galaxies are affected by SMBH feedback in a way that helps to predict higher [α/Fe] ratios and relaxes, but does not yet solve, the problem at high masses. However, little attention is paid to what becomes of the less massive objects which are the building blocks of the relation and responsible for the bulk of the scatter. Suppression of star formation at low and intermediate masses is required in the model.

Interestingly, according to Fig. 10, on average the final [α/Fe] ratio seems to be independent of the the total number of mergers (top panel) as well as of the number of major mergers (bottom panel). Moreover such a relationship also holds if we consider the number of either dry or wet mergers, and is independent of the merger classification[5]. There is a trend such that galaxies with more than ~5 mergers in their formation histories

---

[5] Since gas is always present in the model galaxies, we tested three wet merger definitions – namely when the total mass in gas divided by the total baryon mass of a newly formed galaxy exceed 0.01, 0.05 and 0.1 – and we did not find substantial differences between them. Note that dry mergers are then defined by subtracting the number of wet mergers to the total for a given galaxy.

always have relatively high α/Fe ratios. As the most massive galaxies are those which underwent the highest number of both total and wet mergers in their lifetime, these objects display relatively high α/Fe ratios and old ages. If we select again the galaxies with SSP-weighted ages larger than 10 Gyr, we find that all the galaxies with a number of mergers larger than 7 belong to this category. (Not) surprisingly they are also the most massive (stellar masses larger than $5 \times 10^{11} M_\odot$). This is because larger haloes are the first to form and to reach the mass where the feedback turns on. The majority of galaxies with a number of mergers in their lifetime lower than 4 (2) have formation epochs larger than 1 (2) Gyr, and have mostly stellar masses smaller than 2 (1) $\times 10^{11} M_\odot$.

The model predicts a lot of galaxies that underwent 0 mergers which exhibit a large scatter in the final [α/Fe] ratio. These are galaxies which evolve from disc to bulge morphology through instabilities at late times, but keep a non-negligible disc component (i.e. they have $0.219 < I < 0.01$). These galaxies have masses below $10^{11} M_\odot$ and are satellites (crosses, upper panel of Fig. 3). If they are located in environments where the AGN-quenching threshold occurs too late, they will populate the [α/Fe]-mass plane at values lower than the observed ones. In this case a better treatment of the feedback at galactic scales, possibly including (SNIa-driven) winds, might represent a solution. On the other hand, small galaxies in environments where the AGN-quenching threshold occurs too early and that did not merge to form the most massive spheroids, will populate the [α/Fe]-mass plane at values higher than the observed ones. We argue that this may be a common feature in the most recent models available in the literature. For instance, Kimm et al. (2009), compared five different galaxy formation models to recent observations and found that all of them over predict the fraction of red and passive satellite galaxies. Fontanot et al. (2009) argue that this problem is linked to excessively efficient formation of central galaxies in high redshift haloes. The existence of such a problem in models in which most of the galaxy assembly occurs via dry mergers has been foreseen on more general grounds by PM08 by means of simple arguments which do not depend on processes as feedback or merger history. In a sense one could turn the argument around and say that a robust prediction of semi-analytic models of hierarchical galaxy formation is the presence of low-mass, highly [α/Fe]-enhanced satellite galaxies at high redshift because it is the only way in these models to build local massive ellipticals with the observed [α/Fe] ratios. We know from observations that such objects do not seem to exist at moderately high redshifts around $z \sim 0.4$ (Ziegler et al. 2005). One interesting (but probably not unique) possibility is if these systems accrete some fresh gas over a long time-scale to keep SF going and, therefore, decrease the [α/Fe] ratio. Alternatively, as suggested by Font et al. (2008 – but for a different galaxy formation model), a less aggressive role of the environment (e.g. ram-pressure stripping) may leave more gas in the satellite galaxies.

In conclusion, for the most massive spheroids, the interplay between the peak in the merger rate and the subsequent AGN quenching of the star formation act together in such a way that most of the star formation process and the galactic assembly occur at roughly the same time and the same place, thus mimicking a sort of "monolithic" behaviour. In other words, even though the duration of the star formation would lead to quite low [α/Fe] ratios from the point of view of a pure chemical evolution model, the fact that this happened in several sub-units makes the final [α/Fe] ratios higher and in better agreement with observations. Intermediate and small objects, instead, do not have a quenching

mechanism acting directly at the scales which can self-regulate the duration of the star formation. Therefore they end up having either too high or too low [α/Fe] ratios.

In order to improve the agreement between predictions and observations, we modified the model by modifying the other source of feedback present in GalICS, namely the SN feedback, by changing the efficiency of mass–loading during the triggering of a galactic wind by SNII explosions. Increasing ϵ in Eq. (7) produces more feedback, heating more cold gas, ejecting more hot gas from haloes, and thus reduces the amount of gas that can potentially form stars. In this case, we find that the predicted stellar masses are smaller than in the fiducial case. The galaxies look slightly more α-enhanced as expected since the SF process is strongly disfavoured by the SNe explosions. However, this is not a viable solution for the α/Fe-mass relation problem, since the high mass-loading also implies a very low metal content in the stars. The predicted MMR is offset downwards by at least 0.5 dex from the observational one. On the other hand, if we switch the SN feedback off, we tend to slightly worsen the α/Fe-mass relation, whereas the agreement for the MMR improves.

Following the above line of thoughts, we further modify GalICS by introducing SNIa contributions into Eq. (7). Since α elements and Fe are still ejected at the same rate, this change has the same effects of increasing ϵ[6]. A 0.1 dex increase in the final [α/Fe] ratios can be achieved when a differential wind is invoked, namely if we assume that twice more Fe than O can be ejected in the hot phase due to SNIa explosions. Again, given the nature of such a mechanism, neither the slope of the predicted α/Fe-mass relation can be steepened nor its scatter reduced. Further investigation will tell us if a change in the SNe feedback, namely by allowing them to quench the star formation as in monolithic numerical simulations (e.g. Pipino et al. 2008, 2009), might be the required galactic scale source of feedback.

7. Conclusions

We implemented a detailed treatment for the chemical evolution of H, He, O and Fe in GalICS, a semi-analytical model for galaxy formation which successfully reproduces basic low and high redshift galaxy properties. The contribution of supernovae (both type Ia and II) as well as low and intermediate mass stars to chemical feedback is taken into account.

As expected from chemical evolution studies, it is the shape of the SFH which sets the final [α/Fe]: a galaxy with a shorter duration of the SFH (summed over all the progenitors) will have a higher [α/Fe] than a galaxy with a longer one, even if the latter had fewer mergers. Moreover the [α/Fe] values achieved by the galaxies are in general 0.1−0.3 higher than expected by feeding the integral SFH in a pure chemical evolution model. This happens because in GalICS galaxies do not evolve as closed boxes.

The model predictions are compared to the most recent observational results by Thomas et al. (2007). The model shows significant improvement at the highest masses and velocity dispersions with respect to the earlier (albeit not the same) model by Thomas (1999), where the predicted [α/Fe] ratios are now marginally consistent with observed values. This is due to the fact that much attention has been paid to the predicted star formation histories of central galaxies. The latest semi-analytical models, in fact, predict their stars to be on average older than their low mass counterparts. Efficient and early star formation

of their progenitors make massive galaxies red and α-enhanced. However, we find that this chemically improved GalICS still does not produce the overall observed mass and σ-[α/Fe] relations. The slope is too shallow and the scatter too large, in particular in the low and intermediate mass range. Moreover, an excess of low-mass ellipticals with too high a [α/Fe] ratio is predicted. This latter result agrees with the recent finding that several other (independently-developed) galaxy formation models exhibit far too many red and passive satellite galaxies.

We suggest that the failure to reproduce the mass- and σ-[α/Fe] relations can partly be attributed to the way in which star formation and feedback are currently modelled. The merger process is responsible for part of the scatter. We suggest that the next generation of semi-analytical models should feature, especially in the low and intermediate mass range, stellar (SNIa?) feedback mechanisms linked to the star formation history of single galaxies and not only to their host halo properties. This modification to the current implementation of the galaxy formation process in the CDM scenario should be pursued in order to halt late-time star formation in intermediate mass ellipticals. In particular, we showed that an increase in the star formation efficiency and Fe-enhanced winds driven by the SNIa activity may play a role in removing galaxies with too low [α/Fe] ratios. However, given the way they act on galaxy evolution, these effects cannot be effective in either making the slope of the predicted α/Fe-mass relation steeper or in reducing its scatter. In particular, it seems hard to get rid of the low mass galaxies which are too α-enhanced. To reduce the number of such low mass red satellites, other mechanisms, (e.g. Font et al. 2008) should also be implemented.

Furthermore, a drawback of the model is the fact that the MMR cannot be fit simultaneously. In fact, the AGN quenching that alleviates the problems in the σ-[α/Fe] relation at high masses seems to erase the slope in the MMR. Both effects can be explained by the fact that the model is still lacking a quasi-*monolithic* formation for all of the spheroids, which is needed in order to reproduce the α/Fe-mass relation and the MMR at the same time.

References

Athannasoula, E. 2008, MNRAS, 390, 69
Baugh, C. M., Cole, S., & Frenk, C. S. 1996, MNRAS, 283, 1361
Baldry, I. K., Glazebrook, K., Brinkmann, J., et al. 2004, ApJ, 600, 681
Bender, R., Burnstein, D., & Faber, S. M. 1993, ApJ, 411, 153
Bernardi, M., Nichol, R. C., Sheth, R. K., Miller, C. J., & Brinkmann, J. 2006, AJ, 131, 1288
Bower, R. G., Lucey, J. R., & Ellis, R. S. 1992, MNRAS, 254, 589
Bower, R. G., Benson, A. J., Malbon, R., et al. 2006, MNRAS, 370, 645
Bundy, K., Ellis, R. S., & Conselice, C. J. 2005, ApJ, 625, 621
Carollo, C. M., Danziger, I. J., & Buson, L. 1993, MNRAS, 265, 553
Cattaneo, A., Blaizot, J., Devriendt, J., & Guiderdoni, B. 2005, MNRAS, 364, 407
Cattaneo, A., Dekel, A., Faber, S. M., & Guiderdoni, B. 2008, MNRAS, 389, 567
Cimatti, A., Daddi, E., & Renzini, A. 2006, A&A, 453, 29
Cole, S., Aragon-Salamanca, A., Frenk, C., Navarro J., & Zepf, S. 1994, MNRAS, 271, 781
Croton, D. J., Springel, V., White, S. D. M., et al. 2006, MNRAS, 365, 11
Davies, R. L., Sadler, E. M., & Peletier, R. F. 1993, MNRAS, 262, 650
Dekel, A., & Silk, J. 1986, ApJ, 303, 39
De Lucia, G., Springel, V., White, S. D. M., Croton, D., & Kauffmann, G. 2006, MNRAS, 366, 499
Faber, S. M. 1973, ApJ, 179, 423
Font, A. S, Bower, R. G., McCarthy, I. G., et al. 2008, MNRAS, 389, 1619

---

[6] With the obvious difference that we can have ejection of matter also when the SF is zero, because of the nature of SNIa progenitors.

Fontanot, F., Monaco, P., Silva, L., & Grazian, A. 2007, MNRAS, 382, 903
Fontanot, F., De Lucia, G., Monaco, P., Somerville, R. S., & Santini, P. 2009, MNRAS, 397, 1776
François, P., Matteucci, F., Cayrel, R., et al. 2004, A&A, 421, 613
Ferrarese, L., & Merritt, D. 2000, ApJ, 539, L9
Gallazzi, A., Charlot, S., Brinchmann, J., & White, S. D. M. 2006, MNRAS, 370, 1106
Granato, G. L., De Zotti, G., Silva, L., Bressan, A., & Danese, L. 2004, ApJ, 600, 580
Gebhardt, K., Bender, R., Bower, G., et al. 2000, ApJ, 539, L13
Graves, G. J., Faber, S. M., Schiavon, R. P., & Yan, R. 2007, ApJ, 671, 243
Greggio, L. 2005, A&A, 441, 1055
Guiderdoni, B., Hivon, E., Bouchet, F. R., & Maffei, B. 1998, MNRAS, 295, 877
Hasinger, G., Miyaji, T., & Schmidt, M. 2005, A&A, 441, 417
Hatton, S., Devriendt, J. E. G., Ninin, S., et al. 2003, MNRAS, 343, 75 (Paper I)
Hernquist, L. 1990, ApJ, 356, 359
Humphrey, P. J., Buote, D. A. Gastaldello, F., et al. 2006, ApJ, 646, 899
Iwamoto, K., Brachwitz, F., Nomoto, K., et al. 1999, ApJS, 125, 439
Kauffmann, G. 1996, MNRAS, 281, 487
Kauffmann, G., & Charlot, S. 1998, MNRAS, 294, 705
Kauffmann, G., & White, S. D. M. 1993, MNRAS, 261, 921
Kaviraj, S., Devriendt, J. E. G., Ferreras, I., & Yi, S. K. 2005, MNRAS, 360, 60
Kaviraj, S., Schawinski, K., Devriendt, J. E. G., et al. 2007, ApJS, 173, 619
Keres, D., Katz, N., Weinberg, D. H., & Dave', R. 2005, MNRAS, 363, 2
Khochfar, S., & Burkert, A. 2003, ApJ, 597, L117
Kimm, T., Somerville, R. S., Yi, S. K., et al. 2009, MNRAS, 394, 1131
Kroupa, P. 2007 [arXiv:astro-ph/0703124]
Matteucci, F. 1994, A&A, 288, 57
Matteucci, F., & Greggio, L. 1986, A&A, 154, 279
Matteucci, F., & Recchi, S. 2001, ApJ, 558, 351
Matteucci, F., Panagia, N., Pipino, A., et al. 2006, MNRAS, 372, 265
Mannucci, F., Maoz, D., Sharon, K., et al. 2007, MNRAS, 383, 1121
Mehlert, D., Thomas, D., Saglia, R. P., Bender, R., & Wegner, G. 2003, A&A, 407, 423
Merlin, E., & Chiosi, C. 2006, A&A, 457, 437

Mo, H. J., Mao, S., & White, S. D. M. 1998, MNRAS, 295, 319
Nagashima, M., Lacey, C. G., Okamoto, T., et al. 2005, MNRAS, 363, L31
Nesvadba, N. P. H., Lehnert, M. D., Eisenhauer, F., et al. 2006, Apj, 650, 693
Nelan, J. E., Smith, R. J., Hudson, M. J., et al. 2005, ApJ, 632, 137
Peebles, P. 1982, ApJ, 263, L1
Pipino, A., & Matteucci, F. 2004, MNRAS, 347, 968 (PM04)
Pipino, A., & Matteucci, F. 2006, MNRAS, 365, 1114 (PM06)
Pipino, A., & Matteucci, F. 2008, A&A, 486, 763 (PM08)
Pipino, A., Matteucci, F., & Chiappini, C. 2006, ApJ, 638, 739
Pipino, A., D'Ercole, A., & Matteucci, F. 2008, A&A, 484, 679
Pipino, A., Silk, J., & Matteucci, F. 2009, MNRAS, 392, 475
Rawle, T. D., Smith, R. J., Lucey, J. R., & Swinbank, A. M. 2008, MNRAS, 389, 1891
Recchi, S., Matteucci, F., D'Ercole, A., & Tosi, M. 2004, A&A, 426, 37
Recchi, S., Calura, F., & Kroupa, P. 2009, A&A, 499, 711
Renzini, A. 2005, ASSL, 327, 221
Salpeter, E. E. 1955, ApJ, 121, 161
Schawinski, K., Thomas, D., Sarzi, M., et al. 2007, MNRAS, 382, 1415
Schawinski, K., Lintott, C. J., Thomas, D., et al. 2009, ApJ, 690, 1672
Silk, J. 2001, MNRAS, 324, 313
Silk, J. 2005, MNRAS, 364, 1337
Simien, F., & de Vaucouleurs, G. 1986, ApJ, 302, 564
Somerville, R. S., Hopkins, P. F., Cox, T. J., Robertson, B. E., & Hernquist, L. 2008, MNRAS, 391, 481
Springel, V., Frenk, C. S., & White, S. D. M. 2006, Nature, 440, 1137
Strickland, D. K., & Heckman, T. M. 2009, ApJ, 697, 2030
Thomas, D. 1999, MNRAS, 306, 655
Thomas, D., Maraston, C., Bender, R., & Mendes de Oliveira, C. 2005, ApJ, 621, 673
Thomas, D., Maraston, C., Schawinski, K., et al. 2007, IAUS, 241, 546
Trager, S. C., Faber, S. M., Worthey, G., & Gonzalez, J. J. 2000, AJ, 119, 1654
van den Bosch, F. C. 1998, ApJ, 507, 601
Worthey, G., Faber, S. M., & Gonzalez, J. J. 1992, ApJ, 398, 69
Weidner, C., & Kroupa, P. 2005, ApJ, 625, 754
Ziegler, B. L., Thomas, D., Bohm, A., et al. 2005, A&A, 433, 519